Biophysical Chemistry 286 (2022) 106820

Contents lists available at ScienceDirect

Biophysical Chemistry

journal homepage: www.elsevier.com/locate/biophyschem

Citrullination of adenosine deaminase impairs its binding to dipeptidyl peptidase IV

Luiza Karapetyan [a], Svetlana Sharoyan [a], Sona Mardanyan [a], Giulio Lupidi [b], Massimiliano Cuccioloni [c], Mauro Angeletti [c], Shiraz Markarian [d], Hasmik Shilajyan [d], Alvard Antonyan [a,*]

[a] H. Buniatian Institute of Biochemistry of Armenian, NAS, 5/1, P. Sevak Str., Yerevan 0014, Armenia
[b] School of Pharmacy, University of Camerino, via S. Agostino 1, 62032 Camerino, MC, Italy
[c] School of Biosciences and Veterinary Medicine, Via Gentile III da Varano, 62032 Camerino, MC, Italy
[d] Faculty of Chemistry, Yerevan State University, Yerevan, Armenia

ARTICLE INFO

Keywords:
Citrullinated adenosine deaminase
Computational modeling
Electrophoretic mobility
Fluorescence anisotropy
Protein-protein interaction
Resonant mirror biosensor assay

ABSTRACT

The presence of citrullinated adenosine deaminase (ADA) was reported in the synovial fluids of rheumatoid arthritis individuals. This work reports the effects of ADA citrullination on the formation/stabilization of ADA complex with dipeptidyl peptidase IV (DPPIV). The electrophoretic mobility of *in vivo* citrullinated ADA was diminished compared to the native one. The biosensor binding study demonstrated approximately four-fold lower affinity of both *in vivo* and *in vitro* citrullinated ADAs to DPPIV (K_D = 161 ± 51.3 and 171 ± 52.2 nM, respectively) compared with wild ADA (K_D = 38 ± 9.4 nM). These results were confirmed by examining the ADA interaction with DPPIV using size-exclusion chromatography and fluorescence anisotropy methods. The computational modeling of Arg142 → Cit142 modification in ADA showed a local structural rearrangement and a less favorable binding affinity to DPPIV. According to these observations, citrullinated ADA being a possible target triggering autoimmunity hinders also the formation of ADA-DPPIV complex, essential in immune system function.

1. Introduction

Protein citrullination, a post-translational modification of arginine residues to citrulline catalyzed by enzymes of peptidyl arginine deiminase (PAD) family, has become a hot topic of recent research as it is involved in various physiological and pathological processes [1]. This modification decreases the protein positive charge, induces protein conformation changes, and affects the interaction with other proteins, substrates, ligands, eventually disrupting normal protein function.

Citrullination can create unusual epitopes on normal (native) proteins, converting them into 'neo-antigens', which can be targeted by the immune system, triggering an *autoimmune* response [2]. In fact, enhanced PADs' expression and protein citrullination are associated with Alzheimer's and Parkinson's diseases and autoimmune pathologies, such as rheumatoid arthritis (RA), multiple sclerosis, glaucoma, psoriasis, *etc.* [3,4]. Particularly, increased levels and activity of PADs were reported in synovial tissue of RA individuals [5].

The ubiquitous multifunctional enzyme adenosine deaminase (ADA, EC: 3.5.4.4) catalyzes irreversible hydrolytic deamination of adenosine to inosine [6,7]. The enzyme is essential in purine metabolism, development, differentiation, and maturation of lymphoid system, *etc.* [8]. There are two genetically different isoenzymes of ADA – ADA1 and ADA2, with both different catalytic, biochemical and immunochemical characteristics, different distribution in mammalian tissues. Their pH optimums, substrate binding pockets, substrate and inhibitor affinity differ significantly [9]. ADA2, being a predominant circulating in blood serum and demonstrating some other specific functions [10,11], is responsible for a small share of total ADA activity in mammalian tissues.

ADA1 is responsible for ADA activity in most vertebrate tissues. It is the subject of our study in this paper. Since the purification procedures exclude the presence of ADA2 in the studied preparations, in our manuscript, we used the term ADA for ADA1 without numbering. The

* Corresponding author.
E-mail addresses: biochem@biochem.sci.am (L. Karapetyan), giulio.lupidi@unicam.it (G. Lupidi), massimiliano.cuccioloni@unicam.it (M. Cuccioloni), shmarkar@ysu.am (S. Markarian), biochem@biochem.sci.am (A. Antonyan).

https://doi.org/10.1016/j.bpc.2022.106820
Received 22 December 2021; Received in revised form 11 April 2022; Accepted 12 April 2022
Available online 15 April 2022

low molecular, intracellular form of ADA (iADA) is a catalytically active monomer with molecular mass of 32–42 kDa, whereas the high molecular, extracellular form of the enzyme (eADA, molecular mass of ~ 260 kDa) is a non-covalent complex of iADA with the enzyme dipeptidyl peptidase IV (DPPIV). This complex is present in mammalian tissues both in circulating biological fluids and cell membrane-localized forms [12,13]. ADA activity enhances in biological fluids at various pathological situations. The evaluation of its level, an ADA-test, is considered as a reasonable approach in diagnosing several diseases (reviewed in [14]).

Earlier, we observed the statistically significant ($p < 0.0001$) increase of ADA level in synovial fluids (SF) from patients with RA compared to osteoarthritis [15]. The positive correlation of the total ADA activity and iADA/eADA ratio in RA SF was registered too [16]. We have shown that an increase in ADA activity in RA SF was accompanied by the accumulation of iADA, which was negligible in the cases of gout, ankylosing spondylitis, juvenile idiopathic and reactive arthritis. High ADA activity in SFs of these four types of arthritis was accompanied with accumulation of eADA [17]. Multiple analyses elucidated that in SFs of RA, iADA was citrullinated, whereas eADA samples from SFs of all the studied types of arthritis (including RA) did not reveal any protein citrullination [18].

Therefrom, we suggested that citrullination of iADA may interfere in its binding to DPPIV and, consequently, with the stability of ADA-DPPIV complex.

Structurally, 5 out of 17 arginine residues of human iADA are part of the binding interface to DPPIV. Three of these five, namely, Arg76, Arg81 and Arg142, are actively involved in this interaction [19]. Moreover, Arg142 was shown to be critical in the formation/stabilization of the complex [20]. Hence, it is reasonable to suppose that citrullination of some Arg residues located at the interface of iADA (Arg142, in particular) could hinder its interaction with DPPIV and transformation to eADA, leading to the registered accumulation of iADA in RA SFs.

This work compares the binding of DPPIV to citrullinated and non-citrullinated forms iADA using various techniques.

The results of the study unequivocally evidence the impeding role of ADA citrullination in the formation of ADA-DPPIV complex.

2. Materials and methods

2.1. Materials

The synovial fluids from the knee joints of RA-diagnosed patients were provided by the "Nairi" Medical Center, and the samples were stored at −20 °C until use. Adenosine, peptidylarginine deiminase (PAD2), N-(iodoacetylaminoethyl)-5-naphthylamine-1-sulfonic acid (1,5-IAEDANS), L-citrulline, diacetylmonoxime (DAMO) and thiosemicarbazide (TSC) were purchased from Sigma-Aldrich Ltd. (USA). Molecular weight markers for electrophoresis: bovine serum albumin (BSA), ovalbumin (Ova) and chymotrypsinogen A (CTA) were obtained from Serva (Germany); Sephadex gels – from Pharmacia Biotech (Sweden); and DEAE-cellulose – from Whatman (England). All reagents were of the highest purity available.

2.2. Equipment

Comparative binding experiments were performed on IAsys+ resonant mirror biosensor (Affinity Sensors – Cambridge, UK), equipped with carboxylate cuvettes (Neosensors - Crewe, UK). UV-VIS measurements were carried out on the Cary 60 spectrophotometer (USA). Fluorescence spectra were obtained on Varian-Cary Eclipse PC Varian (USA) spectrofluorometer in standard rectangular quartz cuvettes with light paths of 0.5 and 1 cm. The Bio-Rad PowerPac™ Basic equipment was used for all PAGE electrophoresis procedures.

2.3. Purification of ADA and DPPIV

In our previous works, the chromatographic procedures for isolation and purification of ADA from bovine lung (ADA_{NAT}) [21] and ADA_{SF} from SF of RA patients [18], as well as ADA activity assays were described.

DPPIV purification from bovine kidney to electrophoretic purity and its enzymatic activity assay were described too [22].

2.4. ADA citrullination in vitro

$ADA_{NAT,}$ purified from bovine lung, was citrullinated *in vitro* as described in [23,24]. Briefly, 2 mL of the reaction mixture contained 100 mM Tris-HCl buffer, pH 7.5, 10 mM $CaCl_2$, 5 mM dithiothreitol, 240 μg of ADA_{NAT} and 67 μg of PAD2. After 3 h incubation, the reaction mixture was passed through Sephadex 75 column to separate *in vitro* modified ADA_{EM}.

2.5. Citrulline determination

Protein citrullination in the samples, hydrolyzed in 4 N HCl, was measured using a colorimetric assay based on the specific reaction of DAMO with ureido group under highly acidic conditions [18,25]. Citrulline was quantified from intensity of its absorbance at 530 nm using commercial L-citrulline as a standard. The level of citrullination was expressed as mol of citrulline per mol of protein.

2.6. Polyacrylamide gel electrophoresis

Native gel electrophoresis was performed in Tris-glycine buffer, pH 8.3, according to the method of Davis et al. [26]. At separate experiments, 3–8 μg protein per gel line was injected. After running, 2 gel lines were separated for staining. The remaining 5 lines were cut into 2 mm slices and imbedded into 350 μL of 10 mM phosphate buffer, pH 7.4, to extract the enzyme. After overnight incubation at 4 °C, the aliquots of the supernatant were assayed for citrullination and ADA activity. In these experiments, ADA activity was evaluated by spectral registration of the enzymatic transformation of Ado to inosine (Ino), using the equation [27]:

$$[\mathrm{Ino}] = \Delta A_{240} / \left(\varepsilon^{\mathrm{ino}}{}_{240} - \varepsilon^{\mathrm{ado}}{}_{240}\right) \quad (1)$$

here, ΔA_{240} is the increase in absorbance, $\varepsilon^{ino}_{240} = 12{,}930\ M^{-1}\ cm^{-1}$ and $\varepsilon^{ado}_{240} = 5740\ M^{-1}\ cm^{-1}$ are the molar absorption coefficients of Ino and Ado at 240 nm.

The SDS-PAGE in 10% acrylamide under reducing conditions were carried out in accordance with the method of *Laemmli* [28] in Tris-Glycine buffer, pH 8.3, containing 0.1% SDS. The samples in 10 mM Na-phosphate buffer, pH 7.4, were incubated for 5 min in boiling water bath at the presence of 1% SDS and 1% β-mercaptoethanol. Protein standards, BSA (MW = 67 kDa), Ova (MW = 45 kDa) and CTA (MW = 25 kDa) were prepared similarly.

The electrophoresis procedures were performed at running conditions of 100–120 V, 2 h and 25 °C. The gels were stained with 0.3% Coomassie Blue G-250 and washed with 7.5% acetic acid to remove dye.

The molecular mass of ADA was estimated on the basis of a linear relationship of the log molecular mass to the distance migrated in the SDS-PAGE gel.

2.7. Biosensor binding assay

A biosensor-based assay was used to compare the binding ability of $ADA_{NAT,}$ ADA_{SF} and ADA_{EM} to surface-blocked DPPIV. Briefly, the carboxylate surface was activated by addition of an equimolar mixture of N-hydroxysuccinimide and N-ethyl-N-(dimethylaminopropyl) carbodiimide hydrochloride [29]. DPPIV was dissolved in 10 mM CH_3COONa

buffer pH 5, and then anchored to the carboxylic surface. Free carboxylic sites on the sensor surface were deactivated by injection of 1 M ethanolamine, pH 8.5. Finally, in separate experiments, increasing concentrations of ADA forms of interest were added to the DPPIV coated surface, each time following binding kinetics up to equilibrium. Dissociation steps were performed by a single 1 min wash (80 μL) with fresh PBS buffer. DPPIV surface regeneration was achieved by serial PBS washes (the number of washing cycles depending on the interaction strength), each time assessing the recovery of unbound DPPIV baseline prior to any new addition. All the experiments were performed at 25 °C. Raw data were globally fitted to both mono-exponential and bi-exponential models, and the validity of each model to fit time courses was assessed by a standard F-test procedure as reported elsewhere [30].

2.8. Fluorescence anisotropy

The ADA_{SF} and ADA_{NAT} samples were labeled with N-(iodoacetylaminoethyl)-5-naphthylamine-1-sulfonic acid (1,5-IAEDANS) for fluorescence polarization measurements. The protein samples were incubated overnight at room temperature in 10 mM phosphate buffer, pH 7.4 containing thirty-fold molar excess of IAEDANS. The excess of dye was removed from the mixture by gel filtration on Sephadex G-25 column. Equal aliquots of the AEDANS-ADA fractions obtained were incubated for 10 min in the presence of different concentrations of DPPIV. In these samples, the fluorescence of ADA bound AEDANS was registered at excitation and emission wavelengths of 365 and 490 nm, respectively. At the excitations with vertical and horizontal polarized light, the emissions in both the vertical (I_{VV} and I_{HV}) and horizontal (I_{VH} and I_{HH}) orientations were registered. The fluorescence anisotropy was calculated according to the equation [31]:

$$r = (I_{VV} - GI_{VH})/(I_{VV} + 2GI_{VH}) \quad (2)$$

where $G = I_{HV}/I_{HH}$ is the instrument characterizing parameter [32]. The nonlinear regression analysis of Scatchard plots for r values at different DPPIV concentrations was applied to calculate the dissociation constant, K_D, in ADA-DPPIV complexes.

2.9. Gel-filtration chromatography

The samples of constant DPPIV concentration were incubated with increasing concentration of either ADA_{SF} or ADA_{NAT} for 1 h at 20 °C. Sephadex G-200 column (0.9 × 15 cm) was equilibrated with 10 mM phosphate buffer, pH 7.4, containing 0.1 M KCl. 0.2 mL of the mixtures of interest were injected and eluted with the same buffer at room temperature. 0.5 mL fractions were collected and the elution profile was monitored at 280 nm. In the control experiment, an identical procedure was applied to DPPIV sample in the absence of ADA. The DPPIV containing fractions were assayed for ADA enzymatic activity. The increase in ADA activity (A) in the samples with ADA addition with respect to the control (A_o), $A\text{-}A_o$, was used as a value of ADA newly bound to DPPIV. A nonlinear regression analysis of Scatchard plots for the obtained $A\text{-}A_o$ values was applied to calculate K_D in the ADA-DPPIV complexes.

2.10. Statistical analyses

Statistical analyses were performed using InStat software, version 3, for Windows (GraphPadSoftware, Inc., SanDiego, CA, USA). The unpaired two-tailed *t*-test with Welch correction was applied. Results were expressed as mean values ± standard error.

GraFit [33] was used in the nonlinear regression analysis of Scatchard plots for K_D evaluation in the ADA-DPPIV complexes.

3. Results

3.1. Electrophoretic analysis of ADA samples

Native ADA_{NAT} from bovine lung and citrullinated ADA_{SF} from SF of RA patients were purified applying gel-filtration and ion-exchange chromatography techniques (Section 2.3). In the present study, the ADA_{NAT} and ADA_{SF} preparations with the specific activities 380 μmol/min/mg and 50 μmol/min/mg, respectively, were used. The purity of each preparation was assessed by native and SDS-PAGE (Section 2.6). In Fig. 1, A, the native PAGE pattern of ADA_{NAT} consists of three close bands. The same bands also are seen in the pattern of citrullinated ADA_{SF}. However, the main share of this protein preparation moved noticeably slower and appeared above these three bands.

Fig. 1, B shows the SDS-PAGE patterns of ADA_{SF} and ADA_{NAT}, consisting of identical three bands corresponding to molecular masses 42 kDa, 36 kDa and 32 kDa (Fig. 1, C). The first two bands are darker for human ADA_{SF}, while the third one is darker for bovine ADA_{NAT}. The observed differences between the intensities of the bands of human ADA_{SF} and bovine ADA_{NAT} might be due to their genetically different sources. Actually, all the three bands in the SDS-PAGE correspond to the recognized molecular masses for a small isoform of mammalian iADA [34]. The SDS-PAGE patterns in Fig. 1, B confirm closeness of polypeptide molecules constituting ADA_{SF} and ADA_{NAT} samples.

In fact, according to the results of native PAGE, ADA_{SF} and ADA_{NAT} differ greatly in their mobility, supposedly, caused by citrullination. As it was known, in native electrophoresis, the mobility of proteins depends not only on the charge-to-mass ratio, but also on the physical shape and size of the protein.

Fig. 2 shows the results of analyses of ADA activity (Eq. (1)) and protein citrullination in the supernatants, extracted from 2 mm gel slices after native PAGE (Section 2.6).

According to Fig. 2, A, the ADA activity in the range of mobility 3–4 cm corresponds to the three bands of ADA_{NAT} in Fig. 1, A (the diagram shown above).

According to Fig. 2, B, besides the same range of mobility, ADA activity was revealed also in the range of mobility 1.4–2 cm (the main share of ADA_{SF} protein, Fig. 1, A, the diagram shown above). It is worth noting that the main share of ADA_{SF} with low mobility is citrullinated up to 0.08 μmol of citrulline per a slice of gel (Fig. 2, B, dashed line).

A strong concordance between electrophoretic mobility and the degree of structural orders upon protein citrullination has been manifested in the works of van Beers et al. [24] and Tarcsa et al. [35]

To our knowledge, this is the first publication demonstrating crucial decrease of the electrophoretic mobility of protein, with high probability reflecting the changes in the physical shape and size of the *in vivo* citrullinated protein.

3.2. In vitro interaction of DPPIV with ADA

The ability of ADA to bind DPPIV was evaluated in terms of equilibrium dissociation constant, K_D. Specifically, three methods were used to estimate the K_D values of citrullinated and native ADAs binding on DPPIV.

3.2.1. Biosensor binding assays

First, the *in vitro* interactions between DPPIV, purified from bovine kidney, and citrullinated and non-citrullinated ADAs were studied using a resonant mirror biosensor.

In these experiments, the following ADA forms were used: non-citrullinated ADA_{NAT} from bovine lung; the same – citrullinated *in vitro* by PAD2 (ADA_{EM}); *in vivo* citrullinated ADA_{SF} from SF of RA patients. The used samples were characterized with the specific activity of: a) 380 μmol/min/mg for non-citrullinated ADA_{NAT}; b) 307 μmol/min/mg for citrullinated by PAD2 ADA_{EM} and c) 50 μmol/min/mg for ADA_{SF}. The molar ratios of citrulline to ADA_{EM} and ADA_{SF}, determined as

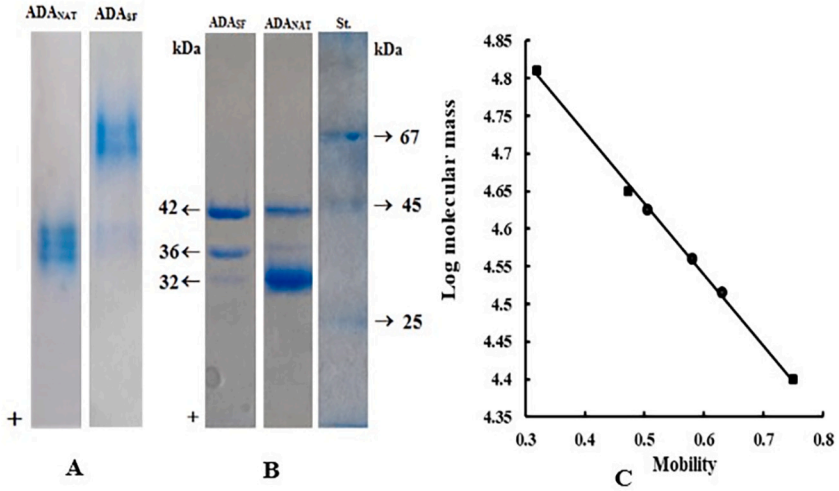

Fig. 1. PAG electrophoresis patterns for wild ADA_{NAT} from bovine lung and citrullinated ADA_{SF} from human SF: A – native PAGE; B – SDS-PAGE of the same samples with a line of standard proteins (St): BSA, 67 kDa; Ova, 45 kDa; CTA, 25 kDa; C – dependence of log molecular mass from mobility for the standard proteins (■) and the ADA preparations (●).

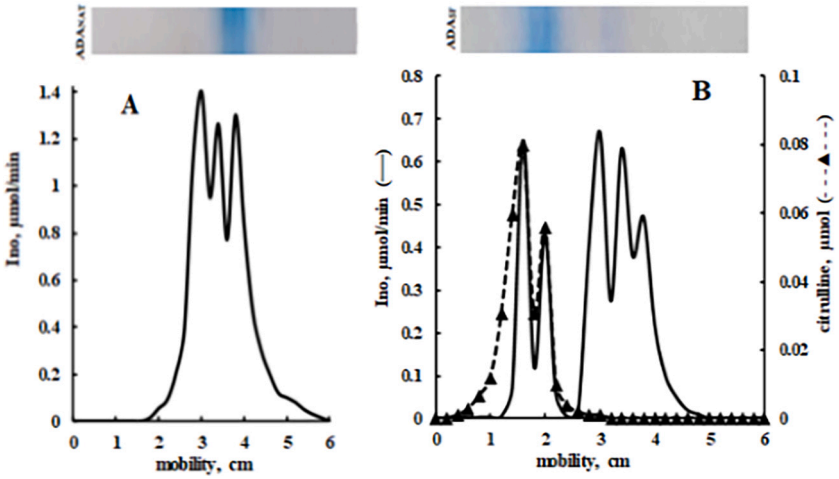

Fig. 2. Diagrams for ADA activity (solid lines) and citrulline (dashed line) in the gel slices after native PAGE for ADA_{NAT} (A) and ADA_{SF} (B).

described in Section 2.5, were 6.35 ± 0.18 mol and 5.8 ± 0.2 mol, respectively. In this work, the SF samples with average value of ADA activity 38-41 U/L were used. The citrullination of iADA depends on the level of ADA activity in SFs at RA, as described in [18] and for this region of ADA activity the number of citrulline per mol of iADA, expressed as A_{530}/A_{280}, is around 5–6, which is in accordance with the value 5.8 ±

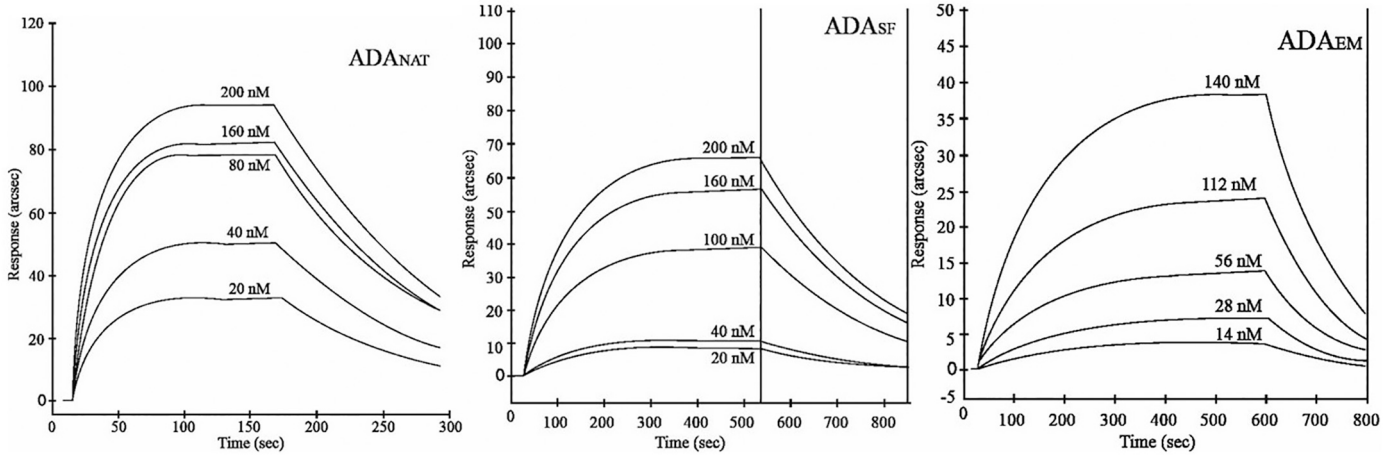

Fig. 3. Representative biosensor responses upon binding of increasing concentrations of the three forms of ADA to surface-blocked DPPIV.

0.2 mol evaluated in the present study.

It must be noted that, the diminished activity upon *in vitro* citrullination of bovine lung ADA in our experiment is in contradiction with the enhanced activity upon *in vitro* citrullination of human recombinant and bovine intestine ADAs, reported by Mitsui and co-authors. This contradiction, namely: activity decreased nearly by 20% in this work and increased by12% (for human recombinant) and 23% (for bovine intestine) reported in [36] might be due to using of both different protein species and assay methods.

In the resonant mirror biosensor experiments, DPPIV was covalently immobilized onto the carboxylate surface of an IAsys+ device (in cuvette concentration = 300 μg/mL) and individually titrated with increasing concentrations of each of ADA forms (Section 2.7). Fig. 3 shows the representative sensorgrams obtained in the experiments. Association and dissociation portions of the binding curves were fitted to both mono- and bi-exponential models: since bi-exponential models did not significantly improve the quality of fits, as judged by standard F-test (95% confidence), the mono-exponential model was used throughout to analyze raw data.

Table 1 summarizes the kinetic and equilibrium parameters for the DPPIV-ADA complex: kinetic and equilibrium parameters (namely k_{ass} and k_{diss}, and K_D, respectively) are presented as mean values of at least three independent experiments ± standard error.

These results evidence the comparable kinetic stability of complexes (k_{diss}) for the three forms of ADA considered. Conversely, k_{ass} values showed similar values for ADA_{SF} and ADA_{EM}, but an approximately ten-fold higher value for ADA_{NAT}, demonstrating a faster recognition process between native ADA and surface blocked DPPIV.

Likewise, the comparison of the affinities of ADAs for DPPIV in terms of K_D ($K_D = k_{diss}/k_{ass}$) proved that the DPPIV-ADA_{NAT} complex was nearly four-fold more stable with respect to complexes involving citrullinated ADAs: K_D values for DPPIV-ADA_{NAT}, DPPIV-ADA_{SF} and DPPIV-ADA_{EM} complexes are 38 ± 9.4, 161 ± 51.3 and 171 ± 52.2 nM, respectively. These results corroborate our hypothesis that citrullination of ADA effectively hinders its binding to DPPIV and, consequently, the formation of DPPIV-ADA complex.

Then, modeling of citrullination of Arg142 from the DPPIV-ADA crystallographic structure was applied, using the Pytms plugin of Pymol [37], followed by energy-minimization with Firedock [38] (Fig. 4).

In agreement with the resonant biosensor data, the modeling resulted in a global structural rearrangement associated with a decreased global energy (mostly attributable to a lower contribution of H-bond to complex stabilization (Table 2).

3.2.2. Fluorescence anisotropy

In the fluorescence anisotropy measurements, interaction of DPPIV, purified from bovine kidney, with IAEDANS labeled ADA_{SF} and ADA_{NAT} samples was studied.

Constant concentrations of IAEDANS labeled ADA_{NAT} (2.3 μM) and ADA_{SF} (2.8 μM), were titrated with increasing concentrations of DPPIV: 0.05–2.0 μM for ADA_{NAT} and 0.1–1.1 μM for ADA_{SF}. For each concentration, the fluorescence emissions of ADA bound AEDANS were registered upon excitations with vertical and horizontal polarized light (as in Section 2.8).

Subsequently, the fluorescence anisotropy was calculated using Eq. (2). Formation of complexes between AEDANS-ADA samples with high molecular DPPIV resulted in the increase of polarization/anisotropy of the AEDANS emission.

K_D values in the DPPIV-ADA complexes were evaluated based on the dependences of anisotropy changes on the increasing concentration of DPPIV. A nonlinear regression analysis of Scatchard plots of obtained data (Fig. 5) yielded the K_D values for ADA_{NAT} and ADA_{SF} samples 54 ± 14 nM and 215 ± 51 nM, respectively. These results corroborate the values get/obtained from the resonant mirror biosensor study (38 ± 9.4 nM and 161 ± 51 nM, respectively).

Table 1
Kinetic and equilibrium parameters for the interactions between the three forms of ADA and the surface-blocked DPPIV.

	k_{ass} ± s.e.m. (M^{-1} s^{-1})	k_{diss} ± s.e.m. (s^{-1})	K_D ± s.e.m. (nM)
ADA_{SF}-DPPIV	25,464 ± 5901	0.0041 ± 0.0009	161 ± 51.3
ADA_{EM}-DPPIV	43,807 ± 13,157	0.0075 ± 0.0004	171 ± 52.2
ADA_{NAT}-DPPIV	209,820 ± 49,150	0.008 ± 0.0006	38 ± 9.4

3.2.3. Size-exclusion chromatography

Afterwards, the formation of DPPIV-ADA complex was investigated using gel-filtration chromatography (Section 2.9.). The mixtures in phosphate buffer, pH 7.4, containing 1 μM DPPIV and increasing concentrations of ADA_{NAT} (from 5 to 250 nM) or ADA_{SF} (from 50 to 1000 nM) were incubated for 1 h at 20 °C. 0.2 mL aliquots of these mixtures were applied to a Sephadex G-200 column. As a control experiment, the same procedure was implemented to the identical preparation of DPPIV without ADA addition. The activities of both of the enzymes in the eluted fractions were determined. The ADA activities in the DPPIV containing fractions in the experiments with ADA addition (A) were compared with those in the control (A_o). The increment of ADA activity in relation to the activity in the control experiment, $A\text{-}A_o$, was used in the nonlinear regression analysis of Scatchard plots (Fig. 6).

In these experiments, the K_D values in the ADA-DPPIV complexes for ADA_{NAT} and ADA_{SF} were evaluated as 49 ± 11 nM and 225 ± 60 nM, respectively. These values are in accordance with the values determined in both the resonant mirror biosensor and the fluorescence polarization studies.

4. Discussion

In human cells, ADA exists mostly as a 32–42 kDa soluble monomer. On the epithelial lymphoid cells and in biological fluids, it is bound to the ADA complexing protein, identified as a T lymphocytes antigen CD26 – membrane glycoprotein ecto-enzyme DPPIV [6–8,12,13]. It was proved that ADA binding to DPPIV/CD26 on dendritic cells enhances T-cells activation and proliferation [39].

The DPPIV binding site of human ADA is localized to the peripheral α2-helix (amino acids 126–143). Glu-139, Arg-142 and Asp-143 in this segment determine the stable binding of ADA to DPPIV. Mutation of all these residues to alanine lowered the affinity of ADA toward DPPIV, increasing the ADA-DPPIV complexes dissociation rates 6–11-fold, and the K_D value – from 17 (for wild type ADA) to 112–160 nM [40].

In the present work, the interaction of bovine DPPIV with three forms of ADA: the purified from bovine lung wild-type ADA_{NAT}, the same, citrullinated *in vitro* by PAD2, ADA_{EM}, and the citrullinated *in vivo* ADA_{SF}, purified from SF of RA patients, was studied. The resonant mirror biosensor, fluorescence anisotropy and gel-filtration methods manifested that the K_D value for DPPIV interaction with two citrullinated forms of ADA is 4-fold higher than the wild type (160–250 nM *versus* 38–54 nM). The similarity of the K_D values for human ADA_{SF} and bovine ADA_{EM} is an expected result, because the DPPIV binding sites on both human ADA [39] and bovine ADA [41] are identical.

For the first time, this work demonstrated the difference in electrophoretic mobility of native ADA and *in vivo* citrullinated ADA_{SF}, namely, the presence of slow mobile bands, exhibiting both ADA activity and citrullination (Fig. 2, B).Similar observation is made by Tarcsa et al. [35], who reported that, after PAD modification of filaggrin and trichohyalin, their mobility progressively slowed down due to the decrease in net charge, loss of potential ionic bonds and interference with H-bonds. The biophysical measurements confirmed that modification of these proteins by PAD reduced the degree of their structural order. Similarly, in the work of van Beers et al. [24], the human fibrinogen was citrullinated *in vitro* by PAD. The analyses by PAGE evidenced

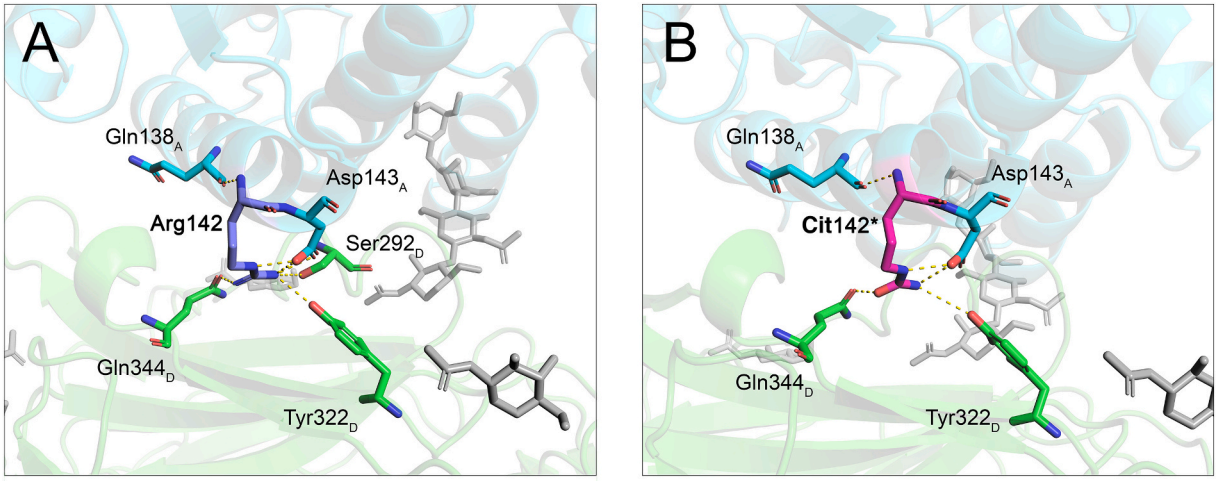

Fig. 4. Comparative visualization of residues in close proximity to Arg142, directly involved in the formation of H-bonds: crystallographic structure (Panel A) and re-modeled structure upon citrullination (Panel B). Residues belonging to ADA and DPPIV are rendered as light blue and green sticks, respectively. H-bonds are indicated as yellow dashed lines. (For interpretation of the references to colour in this figure legend, the reader is referred to the web version of this article.)

Table 2
Energy contribution values for ADA_{NAT}-DPPIV and ADA_{CIT}-DPPIV (Global Energy, the binding energy of the complex; aVdW, rVdW, softened attractive and repulsive van der Waals energy; ACE, atomic contact energy; HB, hydrogen and disulfide bonds).

	Global energy	Attractive VdW	Repulsive VdW	ACE	HB
ADA_{NAT}-DPPIV	−33.11	−45.94	10.64	9.05	−8.16
ADA_{CIT}-DPPIV	−23.68	−35.46	10.46	6.16	0.00

diminished migration of the citrullinated chains of the protein in agreement with the levels of their citrullination.

5. Conclusions

This work manifests the difference in the electrophoretic mobility of wild ADA and *in vivo* citrullinated ADA_{SF}, which can be explained by the change in the charge, conformation and size of protein, caused by the citrullination of arginine residues.

The present work demonstrates that citrullination of ADA directly affects its interaction with DPPIV, which is essential for the formation of ADA-DPPIV complex. We can presume that impairment of citrullinated ADA interaction with DPPIV may lead to failure of the immune system function in autoimmune pathologies, particularly, at rheumatoid arthritis [42,43].

Moreover, the obtained data confirm that, the reduced interaction of iADA with DPPIV due to protein citrullination is the biochemical mechanism of accumulation of iADA in SFs of RA.

The autoantibodies(IgGs) against citrullinated iADA from patients with RA were obtained (by rabbit immunization) and characterized by ELISA assay. It was shown that autoantibodies purified from rabbit plasma were identical to IgGs contained in SFs specific for iADA at RA [unpublished]. Citrullination of ADA and production of autoantibody against it, can serve as a new/early biomarker in the RA diagnosis, making it possible to find new strategies for its prevention/ treatment.

Further studies are needed to better understand the role of ADA in SFs at different stages of RA for developing preventive and/or

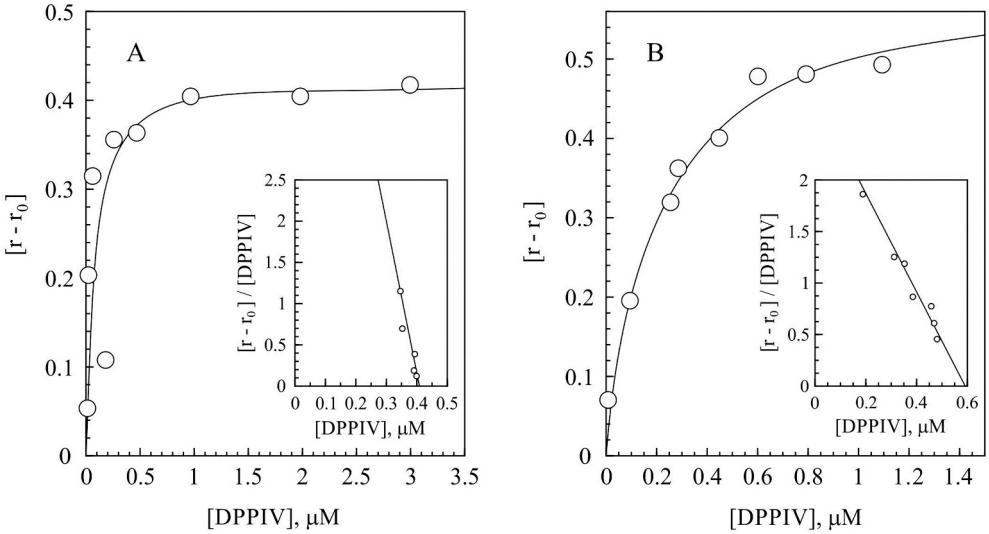

Fig. 5. Dependence of AEDANS-ADA anisotropy changes on the concentration of DPPIV. Inset, the nonlinear Scatchard plots for the fluorescence anisotropy at titration of IAEDANS labeled ADA_{NAT} (A) and ADA_{SF} (B) with increasing concentration of DPPIV.

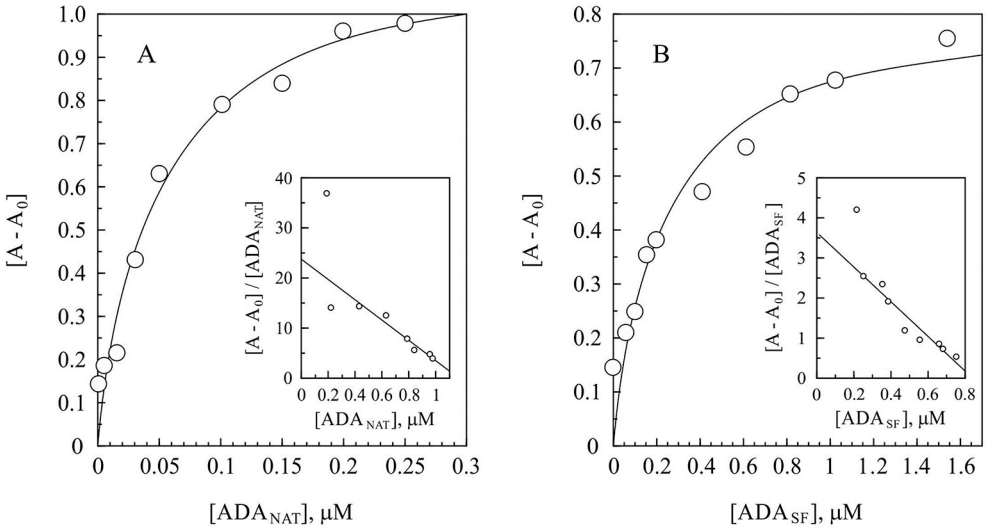

Fig. 6. Dependence of ADA activity increment on the concentrations of ADA_{NAT} (A) and ADA_{SF} (B) in DPPIV-ADA complexes. Inset, the nonlinear Scatchard plots obtained for the results of gel-filtration of the mixtures of 1 μM DPPIV with the varying concentrations of ADA are shown.

therapeutic approaches.

Author statement

The corresponding author, Alvard Antonyan is responsible for ensuring that the descriptions are accurate and agreed by all authors.

Alvard Antonyan and Sona Mardanyan prepared the manuscript and addressed the revision.

Luiza Karapetyan and Svetlana Sharoyan conducted the protein-protein interaction studies.

Giulio Lupidi and Massimiliano Cuccioloni realized the investigations with biosensor resonant technique.

Mauro Angeletti performed the computational molecular modeling.

Shiraz Markarian and Hasmik Shilajyan participated the fluorescence anysotropy research.

Declaration of Competing Interest

The authors have no financial conflicts of interest.

Acknowledgments

The work was supported by a research grant awarded in 2019 to A. Antonyan by the Armenian National Science and Education Fund (ANSEF, #biochem-5084), and by the Ministry of Education and Science of the Republic of Armenia, Agreement N№ 15.

References

[1] M.-L. Yang, F.M.C. Sodré, M.J. Mamula, L. Overbergh, Citrullination and PAD enzyme biology in type 1 diabetes – regulators of inflammation, Autoimmun. Pathol. Front Immunol. 12 (2021), 678953, https://doi.org/10.3389/fimmu.2021.678953. eCollection.

[2] A.D. Fox, Citrullination: a specific target for the autoimmune response in rheumatoid arthritis, J. Immunol. 195 (2015) 5–7, https://doi.org/10.4049/jimmunol.1501021.

[3] M. Alghamdi, D. Alasmari, A. Assiri, E. Mattar, A.A. Aljaddawi, S.G. Alattas, E. M. Redwan, An overview of the intrinsic role of citrullination in autoimmune disorders, Rev. Article J. Immunol. Res. 2019 (2019) 1–39, https://doi.org/10.1155/2019/7592851. Article ID 7592851.

[4] Z. Baka, B. Gyorgy, P. Geher, E.I. Buzas, A. Falus, G. Nagy, Citrullination under physiological and pathological conditions, Joint Bone Spine 79 (2012) 431–436, https://doi.org/10.1016/j.jbspin.2012.01.008.

[5] D. Damgaard, L. Senolt, C.H. Nielsen, Increased levels of peptidylarginine deiminase 2 in synovial fluid from anti-CCP-positive rheumatoid arthritis patients: association with disease activity and inflammatory markers, Rheumatology (Oxford) 55 (2016) 918–927, https://doi.org/10.1093/rheumatology/kev440.

[6] P.E. Daddona, Human adenosine deaminase, J. Biol. Chem. 256 (1981) 12496–12501 (PMID: 6975278).

[7] M.B. Van der Weyden, W.N., Kelley human adenosine deaminase. Distribution and properties, J. Biol. Chem. 251 (1976) 5448–5456 (PMID: 9388).

[8] J. Kameoka, T. Tanaka, Y. Nojima, S. Schlossman, C. Morimoto, Direct association of adenosine deaminase with T cell activation antigen, CD26, Science 261 (1993) 466–469, https://doi.org/10.1126/science.8101391.

[9] J.G. Niedzwicki, D.R. Abernethy, Structure–activity relationships of ligands of human plasma adenosine deaminase 2, Biochem. Pharmacol. 41 (1991) 1615–1624.

[10] A.V. Zavialov, A. Engström, Human ADA2 belongs to a new family of growth factors with adenosine deaminase activity, Biochem. J. 391 (2005) 51–57.

[11] A.V. Zavialov, E. Gracia, N. Glaichenhaus, R. Franco, A.V. Zavialov, G. Lauvau, Human adenosine deaminase 2 induces differentiation of monocytes and stimulates proliferation of T helper cells and macrophages, J. Leukoc. Biol. 88 (2010) 279–290.

[12] R.P. Dong, J. Kameoka, M. Hegen, T. Tanaka, Y. Xu, S.F. Schlossman, C. Morimoto, Characterization of adenosine deaminase binding to human CD26 on T cells and its biologic role in immune response, J. Immunol. 156 (1996) 1349–1355 (PMID: 8568233).

[13] A.A. Antonyan, Natural substrates of dipeptidyl peptidase IV, proceedings of the YSU, Chem. Biol. 2 (2016) 33–42.

[14] A. Antonyan, Adenosine deaminase: a target enzyme in differential pathologies - a review, World J. Pharmac. Life Sci. 3 (2017) 6–18.

[15] A.A. Antonyan, A.A. Haroyan, R.A. Harutyunyan, S.G. Sharoyan, S.S. Mardanyan, Adenosine deaminase activity in synovial fluid at arthritis, in: Proceedings of the YSU. Chemistry and Biology 3, 2013, pp. 28–32.

[16] A.A. Antonyan, S.G. Sharoyan, A.A. Haroyan, R.A. Harutyunyan, S.S. Mardanyan, Adenosine deaminase isoforms in synovial fluid at rheumatoid arthritis, in: Proceedings of the YSU. Chemistry and Biology 2, 2014, pp. 54–58.

[17] A. Antonyan, L. Karapetyan, S.G. Sharoyan, S.S. Mardanyan, Isoforms of adenosine deaminase in synovial fluids at different arthritis, Biol. J. Arm. 1 (2017) 92–96, sci. am:238442.

[18] L. Karapetyan, S. Sharoyan, V. Vardanyan, A. Antonyan, S. Mardanyan, Adenosine deaminase in synovial fluid at rheumatoid arthritis is citrullinated, J. Bioch. Mol. Biol. Res. 4 (2019) 225–229.

[19] W.A. Weihofen, J. Liu, W. Reutter, W. Saenger, H. Fan, Crystal structure of CD26/dipeptidyl-peptidase IV in complex with adenosine deaminase reveals a highly amphiphilic Interfac, J. Biol. Chem. 279 (2004) 43330–43335, https://doi.org/10.1074/jbc.M4 05001200E.

[20] F.X. Richard, I. Arredondo-Vega, S.J. Santisteban, D.D. Kelly, M.S. Patel, Hershfield, the binding site of human adenosine deaminase for CD26/dipeptidyl peptidase IV: Arg142Gln mutation impares binding to CD26 but does not cause immune deficiency, J. Exp. Med. 192 (2000) 1223–1236, https://doi.org/10.1084/jem.192.9.1223.

[21] S. Mardanyan, S. Sharoyan, A. Antonyan, A. Armenyan, G. Cristalli, G. Lupidi, Tryptophan environment in adenosine deaminase: enzyme modification with N-bromosuccinimide in the presence of adenosine and EHNA analogs, Biochem. Biophys. Acta 1546 (2001) 185–195, https://doi.org/10.1016/s0167-4838(01)00141-8.

[22] S. Sharoyan, A. Antonyan, S. Mardanyan, G. Lupidi, G. Cristalli, Influence of dipeptidyl peptidase IV on enzymatic properties of adenosine deaminase, Acta Biochim. Pol. 53 (2006) 539–546, https://doi.org/10.18388/abp.2006_3325.

[23] D. Damgaard, L. Senolt, M.F. Nielsen, G.J. Pruijn, C.H. Nielsen, Demonstration of extracellular peptidylarginine deiminase (PAD) activity in synovial fluid of patients

with rheumatoid arthritis using a novel assay for citrullination of fibrinogen, Arthritis Res. Ther. 16 (2014) 498, https://doi.org/10.1186/s13075-014-0498-9.
[24] J.J. van Beers, R. Raijmakers, L.E. Alexander, J. Stammen-Vogelzangs, A. M. Lokate, A.J. Heck, R.B. Schasfoort, G.J. Pruijn, Mapping of citrullinated fibrinogen B-cell epitopes in rheumatoid arthritis by imaging surface plasmon resonance, Arthritis Res. Ther. 12 (2010) R219, https://doi.org/10.1186/ar3205.
[25] T.R. Boyde, M. Rahmatullah, Optimization of conditions for the colorimetric determination of citrulline, using diacetylmonoxime, Anal. Biochem. 107 (1980) 424–431, https://doi.org/10.1016/0003-2697(80)90404-2.
[26] B.J. Davis, Disc electrophoresis - method and application to human serum proteins, Ann. N. Y. Acad. Sci. 121 (2006) 404–427, https://doi.org/10.1111/j.1749-6632.1964.tb14213.x.
[27] H. Pospíšilová, M. Šebela, O. Novák, I. Frébort, Hydrolytic cleavage of N6-substituted adenine derivatives by eukaryotic adenine and adenosine deaminases, in: Bioscience Reports 28, Portland Press, 2008, pp. 335–347, https://doi.org/10.1042/BSR20080081.
[28] U.K. Laemmli, Cleavage of structural proteins during the assembly of the head of bacteriophage T4, Nature 227 (1970) 680–685, https://doi.org/10.1038/227680a0.
[29] R.J. Davies, P.R. Edwards, H.J. Watts, C.R. Lowe, P.E. Buckle, D. Yeung, T. M. Kinning, D.V. Pollard-Knight, The resonant mirror: a versatile tool for the study of biomolecular interaction, Techniq. Protein Chem. 5 (1994) 285–292, https://doi.org/10.1016/B978-0-12-194710-1.50037-0.
[30] M. Cuccioloni, M. Mozzicafreddo, L. Bonfili, V. Cecarini, M. Giangrossi, M. Falconi, S.I. Saitoh, A.M. Eleuteri, M. Angeletti, Interfering with the high-affinity interaction between wheat amylase trypsin inhibitor CM3 and toll-like receptor 4: in silico and biosensor-based studies, Sci. Rep. 7 (2017) 13169, https://doi.org/10.1038/s41598-017-13709-1.
[31] S. Sharoyan, A. Antonyan, S. Mardanyan, G. Lupidi, M. Cuccioloni, M. Angeletti, G. Cristalli, Complex of dipeptidyl peptidase II with adenosine deaminase, Biochem. Mosc. 73 (2008) 943–949, https://doi.org/10.1134/s0006297908080130.
[32] M. Karlsson, U. Carlsson, Protein adsorption orientation in the light of fluorescent probes: mapping of the interaction between site-directly labeled human carbonic anhydrase II and silica nanoparticles, Biophys. J. 88 (2005) 3536–3544, https://doi.org/10.1529/biophysj.104.054809.
[33] R.J. Leatherbarrow, GraFit Version 7, Erithacus Software Ltd., Horley, U.K. GraFit Version 7, Erithacus Software Ltd., Horley, U.K, 2009.
[34] P.E. Daddona, W.N. Kelley, Human adenosine deaminase. Purification and subunit structure, J. Biol. Chem. 252 (1977) 110–115 (PMID: 13062).
[35] E. Tarcsa, L.N. Marekov, G. Mei, G. Melino, S.-C. Lee, P.M. Steinert, Protein unfolding by peptidylarginine deiminase. Substrate specificity and structural relationships of the natural substrates trichohyalin and filaggrin, J. Biol. Chem. 271 (1996) 30709–30716, https://doi.org/10.1074/jbc.271.48.30709.
[36] H. Mitsui, M. Arito, T. Sato, M.K. Yokoyama, N. Suematsu, K. Okamoto, M. S. Kurokawa, K. Yudo, H. Nakamura, M. Beppu, T. Kato, Novel anti-citrullinated peptide autoantibodies identified by proteomics with in vitro citrullinated proteins in patients with rheumatoid arthritis, Inflam. Regener. 33 (2013) 121–130, https://doi.org/10.2492/inflammregen.33.121.
[37] A. Warnecke, T. Sandalova, A. Achour, R.A. Harris, PyTMs: a useful PyMOL plugin for modeling common post-translational modifications, BMC Bioinform. 15 (2014) 370, https://doi.org/10.1186/s12859-014-0370-6.
[38] E. Mashiach, D. Schneidman-Duhovny, N. Andrusier, R. Nussinov, H.J. Wolfson, FireDock: a web server for fast interaction refinement in molecular docking, Nucleic Acids Res. 36 (2008) W229–W232, https://doi.org/10.1093/nar/gkn186.
[39] R. Pacheco, C. Lluis, R. Franco, Role of CD26-adenosine deaminase interaction in T cell-mediated immunity, Inmunología 24 (2005) 235–245.
[40] E. Richard, S.M. Alam, F.X. Arredondo-Vega, D.D. Patel, M.S. Hershfield, Clustered charged amino acids of human adenosine deaminase comprise a functional epitope for binding the adenosine deaminase complexing protein CD26/dipeptidyl peptidase IV, J. Biol. Chem. 277 (2002) 19720–19726, https://doi.org/10.1074/jbc.M111901200.
[41] M.A. Kelly, M.M. Vestling, C.M. Murphy, S. Hua, T. Sumpter, C. Fenselau, Primary structure of bovine adenosine deaminase, J. Pharm. Biomed. Anal. 14 (1996) 1513–1519, https://doi.org/10.1016/0731-7085(96)01845-6.
[42] E. Darrah, F. Andrade, Rheumatoid arthritis and citrullination, Curr. Opin. Rheumatol. 30 (2018) 72–78, https://doi.org/10.1097/BOR.0000000000000452.
[43] W.J. van Venrooij, G.J. Pruijn, How citrullination invaded rheumatoid arthritis research, Arthritis Res. Ther. 16 (2014) 103, https://doi.org/10.1186/ar4458.